AGU PUBLICATIONS

JGR

Journal of Geophysical Research: Oceans

RESEARCH ARTICLE

10.1002/2015JC011576

Swell impact on wind stress and atmospheric mixing in a regional coupled atmosphere-wave model

Lichuan Wu[1], Anna Rutgersson[1], Erik Sahlée[1], and Xiaoli Guo Larsén[2]

[1]Department of Earth Sciences, Uppsala University, Uppsala, Sweden, [2]Wind Energy Department/Resource Assessment Modeling Section, Risø Campus of the Danish Technical University, Roskilde, Denmark

Key Points:
- Adding swell impact on wind stress and atmospheric mixing improves the model performance
- The influence of swell on wind stress is larger than the influence on atmospheric mixing
- The influence of swell on atmospheric mixing and stress should be considered in atmospheric models

Correspondence to:
L. Wu,
wulichuan0704@gmail.com

Citation:
Wu, L., A. Rutgersson, E. Sahlée, and X. Guo Larsén (2016), Swell impact on wind stress and atmospheric mixing in a regional coupled atmosphere-wave model, *J. Geophys. Res. Oceans*, *121*, doi:10.1002/2015JC011576.

Received 18 DEC 2015
Accepted 1 JUN 2016
Accepted article online 6 JUN 2016

Abstract Over the ocean, the atmospheric turbulence can be significantly affected by swell waves. Change in the atmospheric turbulence affects the wind stress and atmospheric mixing over swell waves. In this study, the influence of swell on atmospheric mixing and wind stress is introduced into an atmosphere-wave-coupled regional climate model, separately and combined. The swell influence on atmospheric mixing is introduced into the atmospheric mixing length formula by adding a swell-induced contribution to the mixing. The swell influence on the wind stress under wind-following swell, moderate-range wind, and near-neutral and unstable stratification conditions is introduced by changing the roughness length. Five year simulation results indicate that adding the swell influence on atmospheric mixing has limited influence, only slightly increasing the near-surface wind speed; in contrast, adding the swell influence on wind stress reduces the near-surface wind speed. Introducing the wave influence roughness length has a larger influence than does adding the swell influence on mixing. Compared with measurements, adding the swell influence on both atmospheric mixing and wind stress gives the best model performance for the wind speed. The influence varies with wave characteristics for different sea basins. Swell occurs infrequently in the studied area, and one could expect more influence in high-swell-frequency areas (i.e., low-latitude ocean). We conclude that the influence of swell on atmospheric mixing and wind stress should be considered when developing climate models.

1. Introduction

Surface gravity waves, nearly always present in the air-sea interface, play a vital role in the air-sea interaction. According to their characteristics, surface waves are of two main types: wind sea waves and swell waves. Wind sea waves are waves under the influence of local winds. As waves propagate from their generation areas, they are called swell waves when their peak phase speed (c_p) exceeds the local wind speed. Swell-dominated waves are usually defined as wave age $c_p/U_{10} > 1.2$ or $c_p/u_* > 30$ (U_{10} is the wind speed at 10 m above the sea surface, u_* is the friction velocity). The presence of swell-dominated wave fields is higher than 70% almost everywhere in the global oceans. At low latitudes, swell waves dominate the oceans at almost all times [*Semedo et al.*, 2011]. The existence of swell waves influences the turbulence of the near-surface atmospheric layer and, in turn, the whole atmospheric boundary layer (ABL). Accordingly, swell waves can influence wind stress, wind speed profiles, atmospheric mixing, heat fluxes, etc. [*Veron et al.*, 2008; *Semedo et al.*, 2009; *Carlsson et al.*, 2009; *Högström et al.*, 2009; *Smedman et al.*, 2009; *Rutgersson et al.*, 2012].

Based on the Monin-Obukov similarity theory (MOST), under neutral conditions, the drag coefficient, $C_d = \left(\frac{u_*}{U_{10}}\right)^2$, is usually given by

$$C_{dN} = \left(\frac{\kappa}{ln(10/z_0)}\right)^2 \quad (1)$$

in which, κ is von Karman's constant, $z_0 = \alpha u_*^2/g$ the surface roughness length, α the Charnock coefficient, and g the acceleration due to gravity. Over the ocean, α is found to be related to wave states, i.e., wave age and wave steepness [*Taylor and Yelland*, 2001; *Smedman et al.*, 2003; *Guan and Xie*, 2004; *Drennan et al.*, 2005; *Carlsson et al.*, 2009; *Potter*, 2015]. Under wind wave conditions, the dependence of α on the wave age agrees well with measurements [*Potter*, 2015]. However, under swell conditions, data indicate that the drag

© 2016. American Geophysical Union. All Rights Reserved.

coefficient calculated from the wave-age-dependent Charnock relationship has significant scatter compared with measurements. Many studies demonstrate that the atmospheric turbulence and the drag coefficient are significantly influenced by swell waves [*Drennan et al*., 1999a; *Kudryavtsev and Makin*, 2004; *Högström et al*., 2009]. Measurements and numerical simulations indicate that MOST is invalid under swell conditions [*Drennan et al*., 1999b; *Rutgersson et al*., 2001; *Sullivan et al*., 2008; *Högström et al*., 2013]. Accordingly, the roughness length determined from wind gradients may not have a physical meaning [*Smedman et al*., 2003].

Upward-directed momentum flux has been found under swell conditions, which means that the momentum flux is transferred from the ocean to the atmosphere [*Hanley and Belcher*, 2008; *Sullivan et al*., 2008]. The existence of upward-directed momentum flux may lead to a low-level wind jet, which has been shown in several field measurements and numerical simulations [*Smedman et al*., 1994; *Grachev and Fairall*, 2001; *Sullivan et al*., 2008; *Semedo et al*., 2009]. The atmospheric turbulence over swell is much more complicated than the turbulence over wind waves. The drag coefficient over swell waves is related to other wave parameters in addition to wave age. *Smedman et al*. [2003] found that the drag coefficient was dependent on the value of E_{swell}/E_{wave}, where E_{swell} is the energy of long waves (the phase speed is higher than U_{10}) and E_{wave} is the short wave energy under mixed wind sea/swell wave conditions. The swell contribution to the wind stress can be very significant. For instance, *Sahlée et al*. [2012] found that the drag coefficient is significantly higher than indicated by the results of the COARE 3.0 algorithm [*Fairall et al*., 2003] under wind-following swell conditions. However, *García-Nava et al*. [2009] and *Larsén et al*. [2003] found a reduced drag coefficient under wind-following swell conditions. Under swell conditions, various studies have found the momentum flux to be upward, reduced, or increased compared with under wind sea wave conditions. This indicates the need for an additional parameter capturing the influence of swell. *Högström et al*. [2009] treated the total stress budget under swell conditions as the sum of four terms: (1) the tangential drag contributed by the swell, (2) the remaining tangential drag, (3) the downward momentum flux contributed by the waves moving slower than the wind, and (4) the upward momentum flux contributed by the waves moving faster than the wind. Term (4) can be negative [*Högström et al*., 2015]. Following this idea, *Högström et al*. [2015] calculated the swell peak contribution to the stress as well as the remaining contribution. Using data from three oceanic experiments conducted under near-neutral and moderate wind-following swell conditions, *Högström et al*. [2015] evaluated the contribution of swell peaks and the "residual" drag coefficient, i.e., the part not depending on the waves. The results indicate that the swell peak contribution to the stress is proportional to the swell parameter $H_{sd}^2 n_p^2$, where H_{sd} is the significant swell wave height, n_p is the frequency of the dominant swell, and the "residual" drag coefficient is a linear function of the wind speed only.

Near the surface, the updraughts and downdraughts are affected by the wave characteristics. The atmospheric mixing in the bottom atmospheric layer is directly affected by the waves. The detached eddies from the bottom layer will affect much higher layers [*Nilsson et al*., 2012]. Accordingly, the atmospheric mixing throughout the boundary layer may be affected. From the results of large eddy simulation (LES), *Nilsson et al*. [2012] found that the integral length scale of the vertical wind component increases under wind-following swell conditions, producing more effective mixing in the ABL. Based on the study by *Nilsson et al*. [2012], *Rutgersson et al*. [2012] introduced the swell influence into an $E - l$ turbulence scheme (E is the turbulent kinetic energy and l is the mixing length). In the modified $E - l$ turbulence scheme, a wave contribution parameter is added to the parameterization of the atmospheric mixing length to introduce the enhanced mixing due to swell waves.

Most current atmospheric models exclude the influence of swell on the atmosphere. In this study, we introduce the influence of swell on both atmospheric mixing [*Rutgersson et al*., 2012] and the drag coefficient [*Högström et al*., 2015], separately as well as combined, into a regional atmosphere-wave-coupled system. Based on a 5 year simulation, we study the influence of swell. The rest of the paper is structured as follows: the parameterizations of swell influence on atmospheric mixing and on wind stress are summarized in section 2; the coupled system, experimental design, and measurements used in this study are introduced in section 3; the simulation results are presented in section 4; finally, the discussion and the conclusions are presented in sections 5 and 6.

2. Parameterizations

2.1. Atmospheric Mixing Length

Based on the results of LES, the atmospheric mixing increases under swell conditions compared with the mixing under flat terrain conditions [*Nilsson et al*., 2012; *Rutgersson et al*., 2012]. *Rutgersson et al*. [2012]

modified an $E - l$ turbulence scheme to include the influence of swell on atmospheric mixing through changing the diagnostic length scale, l. The $E - l$ turbulence scheme is based on the turbulent kinetic energy prognostic equation and the diagnostic length scale. The local stability and nonlocal effects are introduced into the mixing length. The length scale is determined by combing two length scales, i.e., l_{up} starting at the surface and l_{down} starting at the top of the mixing domain:

$$\frac{1}{l}=\frac{1}{l_{up}}+\frac{1}{l_{down}} \tag{2}$$

When considering the swell influence, the two length scales are expressed as follows:

$$l_{up}=\int_{z_{bottom}}^{z} F(Ri, c_p/u_*)dz' \tag{3}$$

$$l_{down}=\int_{z}^{z_{top}} F(Ri, c_p/u_*)dz' \tag{4}$$

where z_{bottom} and z_{top} are the lower and upper boundaries of the mixing domain and Ri is the local Richardson number. The function of $F(Ri, c_p/u_*)$ is expressed as

$$F(Ri, c_p/u_*)=\begin{cases}\alpha_n-\frac{2}{\pi}(\alpha_c-\alpha_n)(\alpha_r Ri) & Ri>0\\ \alpha_n-\frac{2}{\pi}(\alpha_c-\alpha_n)arctan(\alpha_r(Ri+W_{mix})) & Ri<0\end{cases} \tag{5}$$

where α_n, α_c, and α_r are coefficients estimated in the original $E - l$ turbulence scheme [*Lenderink and De Rooy*, 2000; *Lenderink and Holtslag*, 2004]. The additional mixing contribution by the waves is indicated by W_{mix}. The criteria for swell influence on atmospheric mixing are as follows:

1. the wave age, c_p/u_*, is higher than 50, i.e., $c_p/u_* > 50$;
2. all wave directions are applied in this new parameterization; and
3. W_{mix} reaches its maximum value (it is treated as 0.5 in this study) under near-neutral conditions ($-1 < Ri < 0$); for conditions under which $-1.5 < Ri < -1$, W_{mix} continuously decreases to 0 based on the idea that the wave-induced mixing vanishes when convection dominates [*Nilsson et al.*, 2012].

2.2. Wind Stress Parameterization

Based on data from several oceanic experiments under wind-following swell conditions during moderate winds, a negative maximum in *uw* cospectra at the frequency of the dominant swell frequency is demonstrated to be linearly related to the square of the wave orbital motion ($1.25H_{sd}^2 n_p^2$) [*Högström et al.*, 2015]. The magnitude of *uw* cospectra peaks corresponding to the contribution of swell on the surface wind stress, is linearly related to the wave parameter, $1.25H_{sd}^2 n_p^2$. The residual wind stress (including all other contributions except swell contribution to the wind stress) is parameterized as $(C_d)_{windsea}U_{10}^2$. The residual drag coefficient is found to be linearly related to U_{10}. The drag coefficient for wind-following swell under neutral conditions is expressed as

$$C_{dN}=\frac{(C_{dN})_{windsea}+(1.25H_{sd}^2 n_p^2)/U_{10}^2}{1+y} \tag{6}$$

where the residual drag coefficient, $(C_{dN})_{windsea}$, is expressed as

$$(C_{dN})_{windsea}=10^{-3}\times(0.105U_{10}+0.167) \tag{7}$$

The swell-related parameter y is evaluated through linear regression using measurements, as follows:

$$y=\begin{cases}0.269-0.126H_{sd} & 0.5m < H_{sd} < 2m\\ 0 & H_{sd} > 2m\end{cases} \tag{8}$$

The criteria of the *Högström et al.* [2015] parameterization are as follows: (1) near-neutral atmospheric conditions, defined as $z_m/|L_{MO}| < 0.1$, where z_m is the measurement height and L_{MO} the Obukhov length; (2) the

wave age, c_p/U_{10}, is greater than 1.2; (3) the angle between wind and swell propagation direction $|\varphi| < 90^o$; (4) the wind speed is in the range $3.5\,\mathrm{m\,s^{-1}} < U_{10} < 10\,\mathrm{m\,s^{-1}}$.

To apply the *Högström et al*. [2015] parameterization to the atmosphere-wave-coupled system, some adjustments are applied:

1. The parameterization is extended to apply to near-neutral and unstable stratification conditions, i.e., $z_m/L_{MO} < 0.15$. The lowest model layer height, z_m, is approximately 32 m, which exceeds the measurement height in *Högström et al*. [2015]; therefore, in the model, the range $z_m/L_{MO} < 0.15$ is treated as holding under near-neutral and unstable stratification conditions.
2. The wind speed range is set to $U_{10} < 10\,\mathrm{m\,s^{-1}}$. When the wind speed is below $3.5\,\mathrm{m\,s^{-1}}$, $(C_{dN})_{windsea}$ is set to constant $(C_{dN})_{windsea}=5.3\times10^{-4}$, which is the wind sea drag coefficient at a wind speed of $3.5\,\mathrm{m\,s^{-1}}$. For the range $U_{10} > 10\,\mathrm{m\,s^{-1}}$, the default parameterization is used.
3. In the *Högström et al*. [2015] parameterization, the value of $H_{sd}^2 n_p^2$ in the data used to derive the parameterization lie within a limited range (see their Figure 13). The validity of the parameterization outside the range of the data used has not been examined and is questionable. To avoid a possibly physical unrealistic value of C_{dN} in the parameterization, when the value of $H_{sd}^2 n_p^2$ exceeds that found in the range of data used by *Högström et al*. [2015], we instead use the maximum value of C_{dN} in the range of the *Högström et al*. [2015] data. Then, C_{dN} cannot exceed the line of $C_{dN}=(0.27\times U_{10}+1.09)\times10^{-3}$ [see *Högström et al*., 2015, Figure 13].

3. Coupled Model and Measurements

3.1. Atmosphere-Wave-Coupled System

3.1.1. RCA

The Rossby Centre Regional Atmospheric Model Version 4 (RCA) is used in the atmosphere-wave-coupled system. The RCA model is a hydrostatic model incorporating terrain-following coordinates and semi-Lagrangian semi-implicit calculation. It was developed at the Swedish Meteorological and Hydrological Institute (SMHI). The $E-l$ turbulence scheme used in the RCA model [*Lenderink and Holtslag*, 2004; *Rutgersson et al*., 2012] is based on the CBR scheme [*Cuxart et al*., 2000]. The parameterization of wind stress used in the RCA model is based on the roughness length, which is expressed as

$$z_0=f(U)\times\alpha\frac{u_*^2}{g}+[1-f(U)]\times0.11\frac{\nu}{u_*} \tag{9}$$

where α is set to 0.0185 in this study, ν is the air kinematic viscosity, and $f(U)$ is a wind speed function responsible for the transition between smooth and rough flows.

The horizontal resolution of RCA is 0.22° spherical with a rotated latitude/longitude grid. There are 40 vertical layers and the lowest model layer is approximately 32 m above the sea level. The time step in this study is 15 min. Boundary and initial field data are ERA-40 data [*Uppala et al*., 2005]. The domain of RCA in the coupled system is represented by a red box in Figure 1.

3.1.2. WAM

The WAM wave model [*WAMDI*, 1988] is used in the atmosphere-wave-coupled system to provide wave information for the RCA model. The domain of WAM is shown in Figure 1 by a blue box. The resolution of WAM is 0.2° and the time step of WAM is 600 s. In the coupling area (the RCA domain), the RCA model provides the wind speed and direction for WAM every half hour. In the area outside the RCA domain, WAM obtains the wind information from ERA-40 every 6 h. In this coupled system, the WAM domain is larger than that used by the study of *Wu et al*. [2015], and the waves generated outside the RCA domain can influence the simulation results.

The differences between the coupled RCA-WAM system used in this study and the one used in *Rutgersson et al*. [2010, 2012] and *Wu et al*. [2015] are as follows: (1) we use the OASIS3-MCT coupler [*Valcke*, 2013] for the communication between RCA and WAM and (2) RCA and WAM exchange information every 30 min instead of every time step.

3.1.3. Experimental Designs

To investigate the swell influence on atmospheric mixing and wind stress in the simulation results, four experiments were designed. The details of the four experiments are shown in Table 1. The four experiments are used for a 5 year simulation (2005–2009).

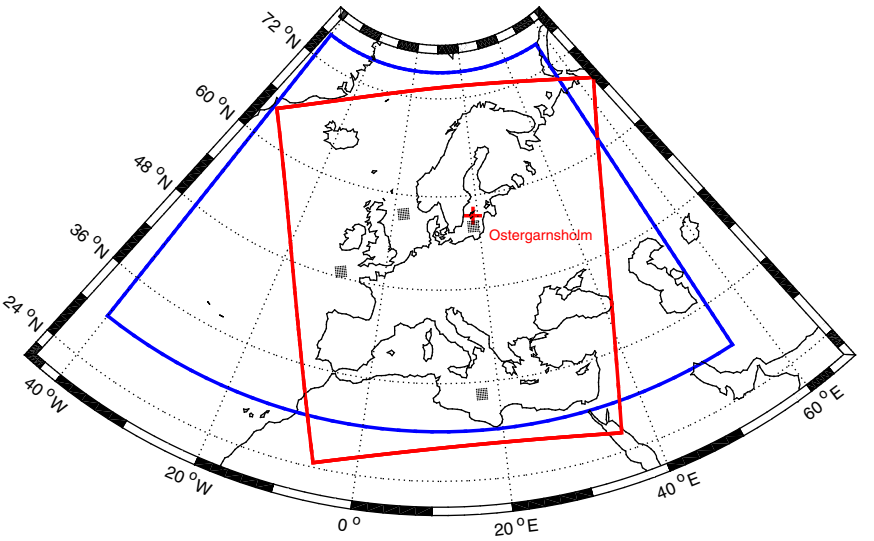

Figure 1. The domain of the coupled system. The blue box is the domain of the WAM model; the red box is the domain of the RCA model. The location of the Östergarnsholm is shown in the figure by red plus sign. The dotted areas represent the four selected areas investigated in detail: the Baltic Sea (BS), the North Sea (NS), Atlantic (AT), and Mediterranean (MT).

Exp-Ctl is the control experiment in which the RCA model provides the wind field for the WAM model, but WAM does not give any wave information to RCA. The Exp-Ctl experiment is used as the reference experiment in undertaking the comparison. In the Exp-Mix experiment, the influence of swell on atmospheric mixing is considered (as explained in section 2.1). The new parameterization of wind stress under wind-following swell conditions is introduced in the Exp-Drag experiment (from section 2.2). In Exp-Drag, the swell-influenced parameterization of the drag coefficient is used to calculate the effective roughness length based on equation (1). In the Exp-Full experiment, the swell influence on atmospheric mixing and the wind stress are both included.

3.2. Measurements

Östergarnsholm is a small flat island with no trees and very sparse vegetation, situated approximately 4 km east of Gotland. A 30 m-high tower is located in southernmost Östergarnsholm (57°27′N, 18°59′E) (see Figure 1), its base approximately 1 m above the sea surface level. The wind speed, wind direction, and temperature are measured at 6.9, 11.8, 14.3, 20, and 28.8 m above the tower base; the humidity is measured at 7 m above the tower base. These meteorological measurements have been made since May 1995. Approximately 4 km southwest of the tower, a directional wave rider (DWR) buoy is used to measure wave parameters (run by the Finnish Meteorological Institute). The depth at the DWR buoy location is 36 m.

The wind data from the 80°–220° sector were used to verify the model performance. Several studies [e.g., *Smedman et al*., 1999; *Högström et al*., 2008] demonstrate that this sector represents open sea conditions in terms of both wave conditions and atmospheric turbulence. During the model simulation comparison, data from this sector were used to exclude data influenced by disturbances from the larger island of Gotland and/or by Östergarnsholm and the 30 m tower. In addition, this choice limits possible influences on the results caused by the low resolution of the model. At this site, 10,597 data points, acquired with a wind speed range of 0.1–18.9 m s^{-1}, are used for comparison with the simulation results.

Table 1. The Experimental Designs for the Comparison: Exp-Ctl is the Control Experiment in Which the RCA Model Provides Only the Wind Information for the WAM Model, Exp-Mix Introduces the Swell Wave Impact on the Atmospheric Mixing, Exp-Drag Introduces the Swell Wave Impact on the Wind Stress, and Exp-Full Includes Both the Swell Impact on Atmospheric Mixing and the Wind Stress

	Atmospheric Mixing Length	Wind Stress Parameterization
Exp-Ctl	Original $E-I$	RCA
Exp-Mix	Modified $E-I$ (section 2.1)	RCA
Exp-Drag	Original $E-I$	Swell impact on wind stress (section 2.2)
Exp-Full	Modified $E-I$ (section 2.1)	Swell impact on wind stress (section 2.2)

4. Results

4.1. Comparison With Measurements

To verify the model performance in term of wind speed, model outputs

Table 2. Statistical Results of the Wind Speed Comparison, i.e., Model Results Versus Measurements at Östergarnsholm: Mean Error (ME, Measured-Modeled) and Its Confidence Level, Mean Absolute Error (MAE), Standard Deviation (STD), Root-Mean-Square Deviation (RMSD), and Correlation Coefficient (R)

	ME	MAE	STD	RMSD	R
Exp-Ctl	−0.685	2.317	2.825	2.906	0.631
Exp-Mix	−0.726 (70%)	2.313	2.821	2.912	0.639
Exp-Drag	−0.629 (80%)	2.338	2.861	2.929	0.635
Exp-Full	−0.607 (95%)	2.280	2.800	2.865	0.642

from the grid points nearest the measurement site are compared with hourly averaged measurements. Five statistical parameters are used in this study: mean error (ME), mean absolute error (MAE), standard deviation (STD), root-mean-square deviation (RMSD), and Pearson correlation coefficient (R).

Table 2 shows statistical results for wind speeds at Östergarnsholm site (10 m). Adding the swell influence on the atmospheric mixing length (Exp-Mix) reduces MAE, STD and RMSD and increases the correlation coefficient. Adding the swell influence on the wind stress (Exp-Drag) improves the simulation results concerning ME of the wind speed. Adding all the wave influences (including atmospheric mixing length and wind stress, Exp-Full) results in the best wind speed performance in the four experiments in terms of ME, MAE, STD, RMSD, and R. The confidence level of ME between the experiments considering swell influence and the control experiment are tested. Although the improvement of ME for the experiments including swell influence is small, there statistical analysis shows the improvement for Exp-Full has passed the 95% confidence level for Östergarnsholm data (Table 2). Compared with Exp-Full, the improvement significant level for Exp-Mix and Exp-Drag are relative lower (70% and 80%, respectively).

To evaluate the model performance for different wind speed ranges, the relative reduced error (RRE) is used. RRE is defined as follows: $RRE_i = (MAE_i - MAE_{ctl})/MAE_{ctl}$, where MAE_{ctl} is the MAE of Exp-Ctl and MAE_i is the MAE of experiment *i*. A negative RRE indicates improved results compared with Exp-Ctl, and a positive RRE indicates reduced agreement with measurements. The RREs of the wind speed simulations at Östergarnsholm site are shown in Figure 2. Adding Exp-Mix or Exp-Drag does not significantly affect the wind simulations. Adding all the swell influences (Exp-Full) results in the best performance at wind speeds below 8 m s^{-1}.

The times when the modeled and measured wind speeds are the same at the Östergarnsholm site are evaluated using 2-D probability density maps, shown in Figure 3a for the control run (Exp-Ctl). If the high probability occurs around the 1:1 line, this means that the model agrees well with the measurements. If the high probability occurs above the line 1:1 line, this means that the model overestimates the wind speed. Similarly, if the probability is high beneath the 1:1 line, this means that the model underestimates the wind speed. One can see that the control simulation (Exp-Ctl) overestimates the wind speed at low wind speeds but underestimates it at high wind speeds. Figures 3c–3e show the probability difference between the three experiments and the control run (Exp-Ctl). If positive probability (red) occurs near the 1:1 line or negative probability (blue) occurs away from the 1:1 line, this means that the model has improved compared with the control run (Exp-Ctl). Adding the swell influence on atmospheric mixing (Exp-Mix) does not have significant influence on the 2-D probability density

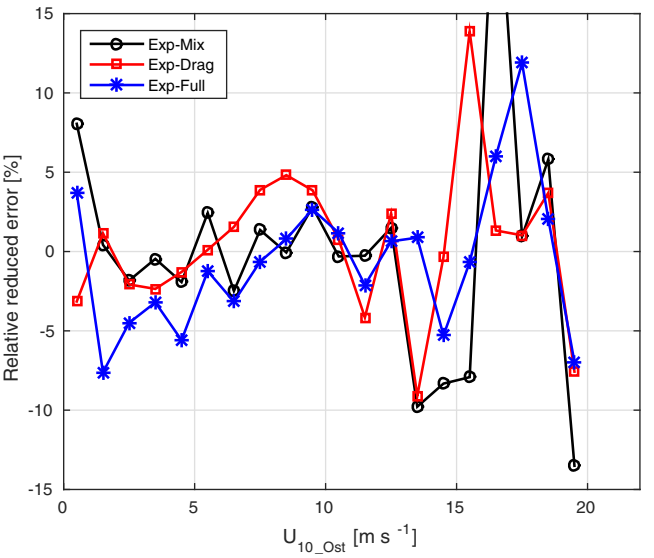

Figure 2. The relative reduced error for different wind bin ranges at Östergarnsholm for wind speed at 10 m.

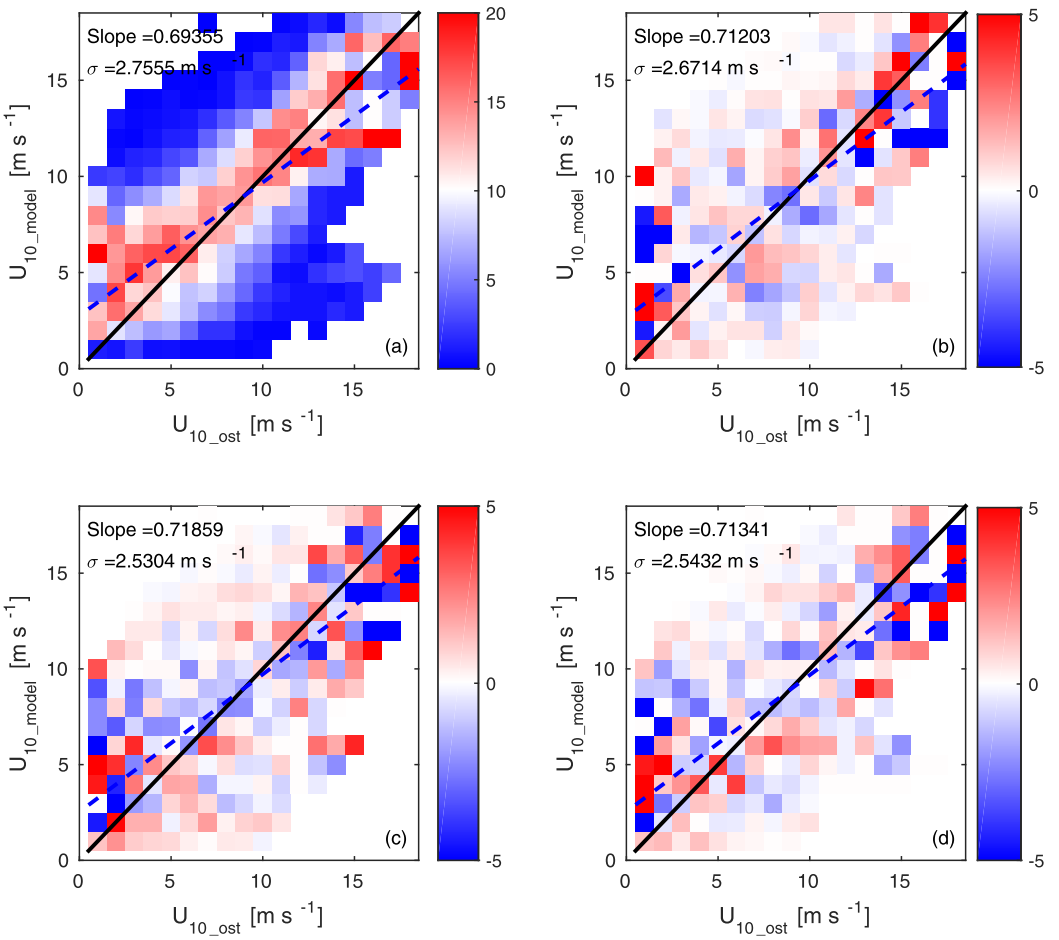

Figure 3. (a) The wind speed simulation percentage distribution at different wind speeds for Exp-Ctl, where the color represents the percentage distribution at a particular wind speed. The solid black line is the 1:1 line; the high percentage around this line indicates that the model simulation is close to the measurements. The dashed blue line is the fitted line. (b) The difference between Exp-Mix and Exp-Ctl, (c) the difference between Exp-Drag and Exp-Ctl, and (d) the difference between Exp-Full and Exp-Ctl.

maps (Figure 3b). Adding the swell influence on the wind stress (Exp-Drag and Exp-Full) reduces the scatter of the simulations at low wind speeds, reducing the overestimation probability but slightly increasing the underestimation probability (see Figures 3c and 3d).

4.2. The Average Influence

The swell probability for Exp-Ctl over the 5 year simulation is shown in Figure 4a. The swell probability in the Atlantic part of the region exceeds 70% in most areas. In the Baltic Sea, the swell probability is lower than in other areas in the domain at approximately 45%. The frequency of occurrence fulfilling the criteria for wave impact on the atmospheric mixing length (i.e., $c_p/u_* > 50$ and $-1 < Ri < 0$) is shown in Figure 4b, with the highest-frequency area in the Atlantic sector and the lowest in the Baltic Sea. The frequency distribution pattern of the condition fulfilling the criteria for wave impact on the atmospheric mixing length is similar to the swell probability distribution (Figure 4a). The frequency of occurrence fulfilling the criteria for swell influence on the wind stress ($U_{10} < 10\,\mathrm{m\,s^{-1}}, |\varphi| < 90^\circ$ and $z_m/L_{MO} < 0.15$) is shown in Figure 4c. The distribution of this frequency of occurrence differs from that of wave impact on the atmospheric mixing length. In the Mediterranean basin, the frequency is higher than in the Atlantic sector, while the Baltic Sea has the lowest probability. The frequency fulfilling the criteria for swell impact on both the wind stress and atmospheric mixing at the same time is shown in Figure 4d, the lowest frequency occurring in the Baltic Sea (below 8%). The frequency in the Atlantic sector is above 16% in most areas. The frequency of occurrence fulfilling the criteria for swell influence on the atmospheric mixing and wind stress varies between sea areas, leading to different influences in different areas.

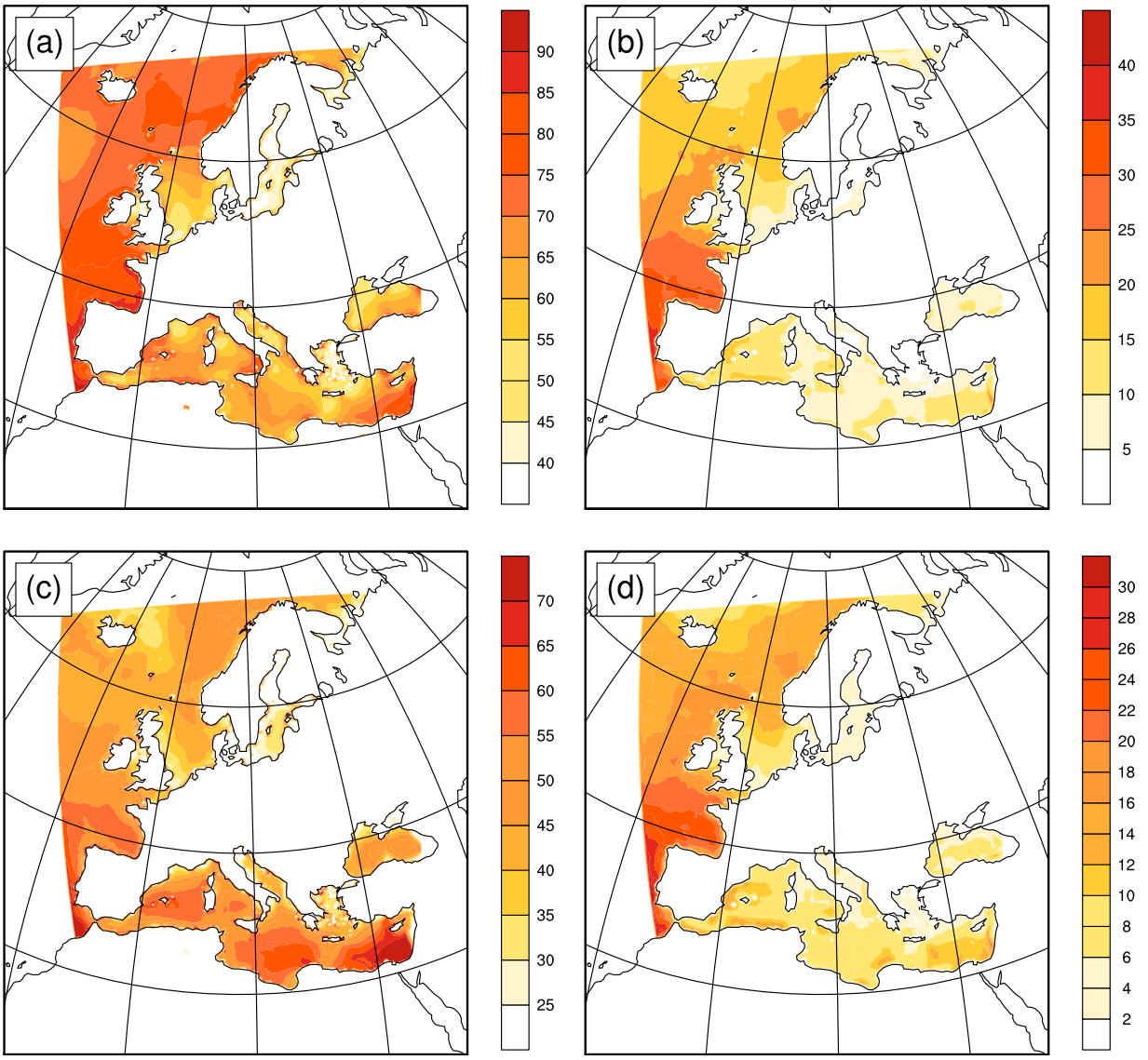

Figure 4. The probabilities (in %) of different parameters for Exp-Ctl: (a) swell probability, (b) the probability satisfying the criteria for the atmospheric mixing parameterization, (c) the probability satisfying the criteria for the wind stress parameterization, and (d) the probability simultaneously satisfying the criteria for the parameterizations of atmospheric mixing and wind stress.

Figures 5 and 6 show the mean difference between the three experiments and the control run (Exp-Ctl) for U_{10} and friction velocity, respectively. Adding the wave impact on atmospheric mixing (Exp-Mix) results in wind speed differences ranging from -0.1 to 0.1 m s^{-1} over ocean on average. In most sea areas, Exp-Mix increases the wind speed in the lower layers, though, the difference varies between sea basins. On average, adding the wave influence on the wind stress (Exp-Drag) reduces the wind speed by more than 0.15 m s^{-1} for the Atlantic Ocean, but by less than 0.05 m s^{-1} for the Baltic Sea. The swell slope in the Baltic Sea is lower than other in the sea basins, resulting in a slight difference in the drag coefficient [*Högström et al.*, 2015, Figure 13]. Adding the wave influence on the atmospheric mixing length and wind stress (Exp-Full) increases the wind speed slightly compared with Exp-Drag; however, it still reduces the wind speed compared with the control run (Exp-Ctl), indicating that the swell impact on the wind stress dominates the swell influences concerning these parameters (Figure 5c). Adding the wave influence on atmospheric mixing (Exp-Mix) slightly increases the friction velocity (Figure 6a) due to the increased wind speed. Adding the wave impact on the wind stress (Exp-Drag and Exp-Full) increases the friction velocity by more than

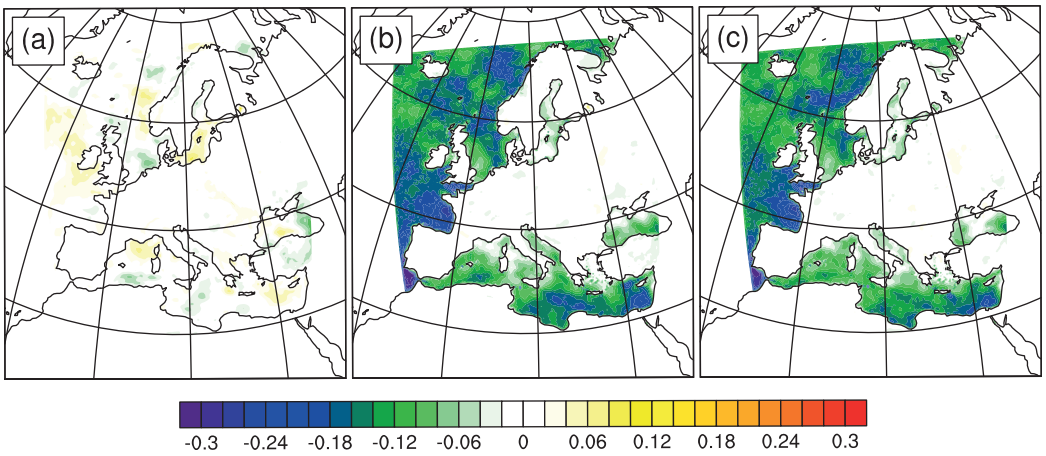

Figure 5. The difference in U_{10} (in m s^{-1}) between the control experiment (Exp-Ctl) and the other experiments: (a) Exp-Mix − Exp-Ctl, (b) Exp-Drag − Exp-Ctl, and (c) Exp-Full − Exp-Ctl.

0.005 m s^{-1} over all seas in general, by more than 0.01 m s^{-1} (4%) in the Atlantic, and by less than 1% in the Baltic Sea.

The swell influences on the simulation results are mainly seen over the sea (Figures 5 and 6). There are also small differences over some land areas concerning U_{10} and u_* when including the swell influences. One possible reason is that the differences of the wind speed caused by swell over the sea changes wind gradients as well as the atmospheric dynamic. Accordingly, it adds secondary impacts also for the friction velocity over land. It should be noted that friction velocities are larger over land and the relative difference over land area are significantly smaller compared with over the sea.

4.3. The Influences on Specific Sea Basins

To study the detailed influences of swell on atmospheric mixing and wind stress under different climatological and environmental conditions, four specific sea basins are chosen, i.e., the Atlantic Ocean (AT), the North Sea (NS), the Mediterranean Sea (MT), and the Baltic Sea (BS) (see Figure 1). To investigate the impact of different parameterizations, only the data fulfilling the criteria of both parameterizations at the same time are used to make the comparisons (see Figures 7–10).

Adding the swell impact on the atmospheric mixing length (Exp-Mix) increases U_{10} in all chosen sea basins. The influence of swell on atmospheric mixing does not have a significant trend relationship with the wave parameter $(H_{sd}n_p)^2$ (see Figures 7a, 8a, 9a, and 10a). However, the increase in U_{10} is mainly under low mixed

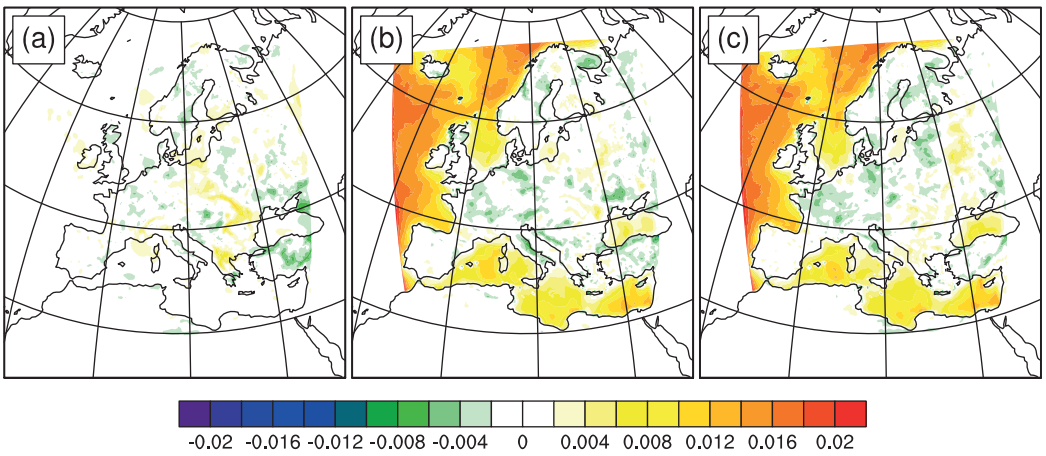

Figure 6. The difference in u_* (in m s^{-1}) between the control experiment (Exp-Ctl) and the other experiments: (a) Exp-Mix − Exp-Ctl, (b) Exp-Drag − Exp-Ctl and (c) Exp-Full − Exp-Ctl.

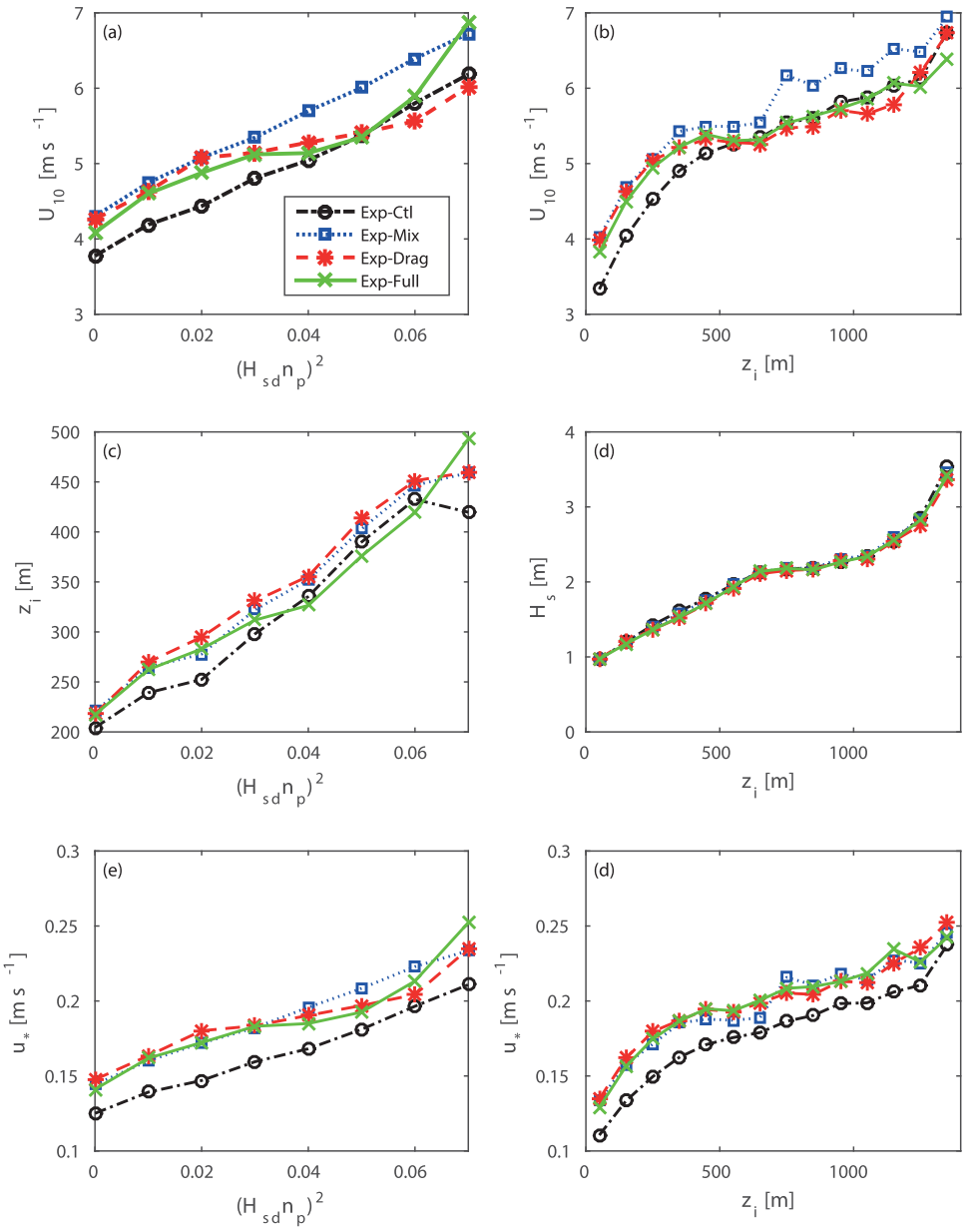

Figure 7. Average over intervals of (left columns) $(H_{sd}n_p)^2$ and (right columns) z_i from the Exp-Ctl simulations: (a, b) U_{10}, (c) z_i, (d) H_s, and (e, f) u_* for the BS in Figure 1. Circles indicate the Exp-Ctl results, rectangles the Exp-Mix results, stars the Exp-Drag results, and crosses the Exp-Ful results. Only data meeting the swell impact criteria for both atmospheric mixing length and wind stress are included.

layer height (MLH) conditions (see Figures 7b, 8b, 9b, and 10b), which is consistent with the finding of *Rutgersson et al*. [2012] that the increase in MLH is mainly in $MLH_{ctl} < 300$ m. The MLH is defined according to the gradient of the virtual potential temperature [*Troen and Mahrt*, 1986]. Adding the swell impact on the wind stress reduces U_{10} in the MT, NS and AT basins. With the increase in MLH, U_{10} decreases more than it does under lower MLH conditions when adding the swell impact on the wind stress (Exp-Drag). With the increase in $(H_{sd}n_p)^2$, the influence of swell on the drag coefficient should increase according to the parameterization of *Högström et al*. [2015, Figure 13]. This trend is found in the Baltic Sea basin, which indicates that the swell increases/decreases U_{10} when $(H_{sd}n_p)^2$ is smaller/lager; however, this trend is not found in other sea basins, possibly because of model feedback influences (the decrease/increase of U_{10} caused by swell changes the wind speed in next model time step, which in turn impacts the wind speed patter satisfied the criteria). In MT, NS, and AT, the occurrence frequency of swell impact on the wind stress is higher,

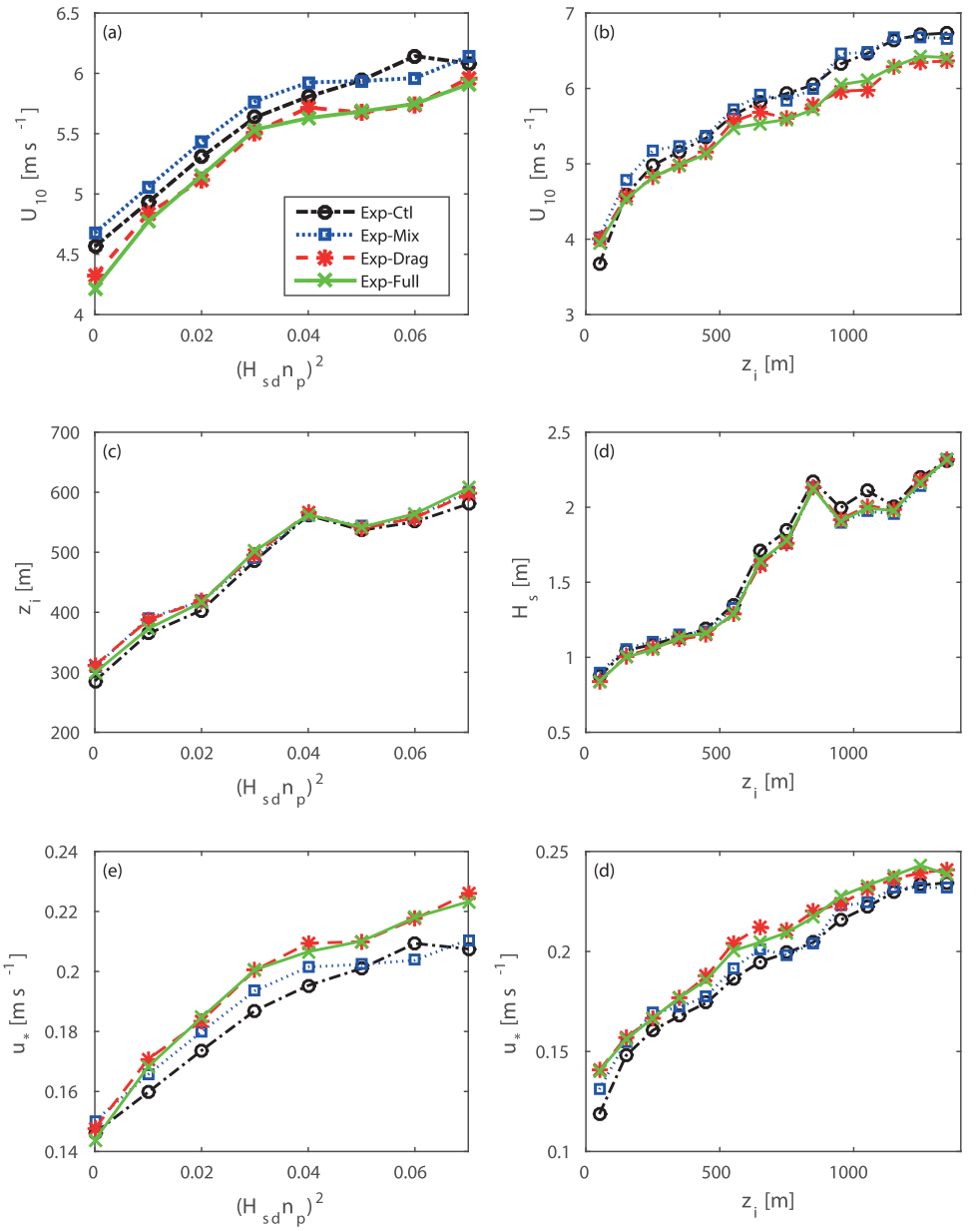

Figure 8. Average over intervals of (left columns) $(H_{sd}n_p)^2$ and (right columns) z_i from the Exp-Ctl simulations: (a, b) U_{10}, (c) z_i, (d) H_s, and (e, f) u_* for the MT in Figure 1. Circles indicate the Exp-Ctl results, rectangles the Exp-Mix results, stars the Exp-Drag results, and crosses the Exp-Ful results. Only data meeting the swell impact criteria for both atmospheric mixing length and wind stress are included.

however, the occurrence frequency of swell impact on the atmospheric mixing length is lower. The combination impact (Exp-Full) is dominated by the wave impact on the wind stress (Exp-Drag).

Both Exp-Mix and Exp-Drag increase the MLH, while, Exp-Full has a smaller impact (see Figures 7c, 8c, 9c, and 10c). Although the influence of swell on the wind stress (atmospheric mixing length) reduces (increases) the wind speed at 10 m, it does not have a significant impact on the simulation results concerning the significant wave height (Figures 7d, 8d, 9d, and 10d).

The influence of waves on the friction velocity with the change in $(H_{sd}n_p)^2$ is shown in Figures 7e, 8e, 9e, and 10e. The influences of waves on both the wind stress (Exp-Drag) and the atmospheric mixing length (Exp-Mix) increase the friction velocity. Although the impact of waves on the wind stress reduces the wind speed, the drag coefficient increases with $(H_{sd}n_p)^2$, leading to an increase in the friction velocity. In the NS

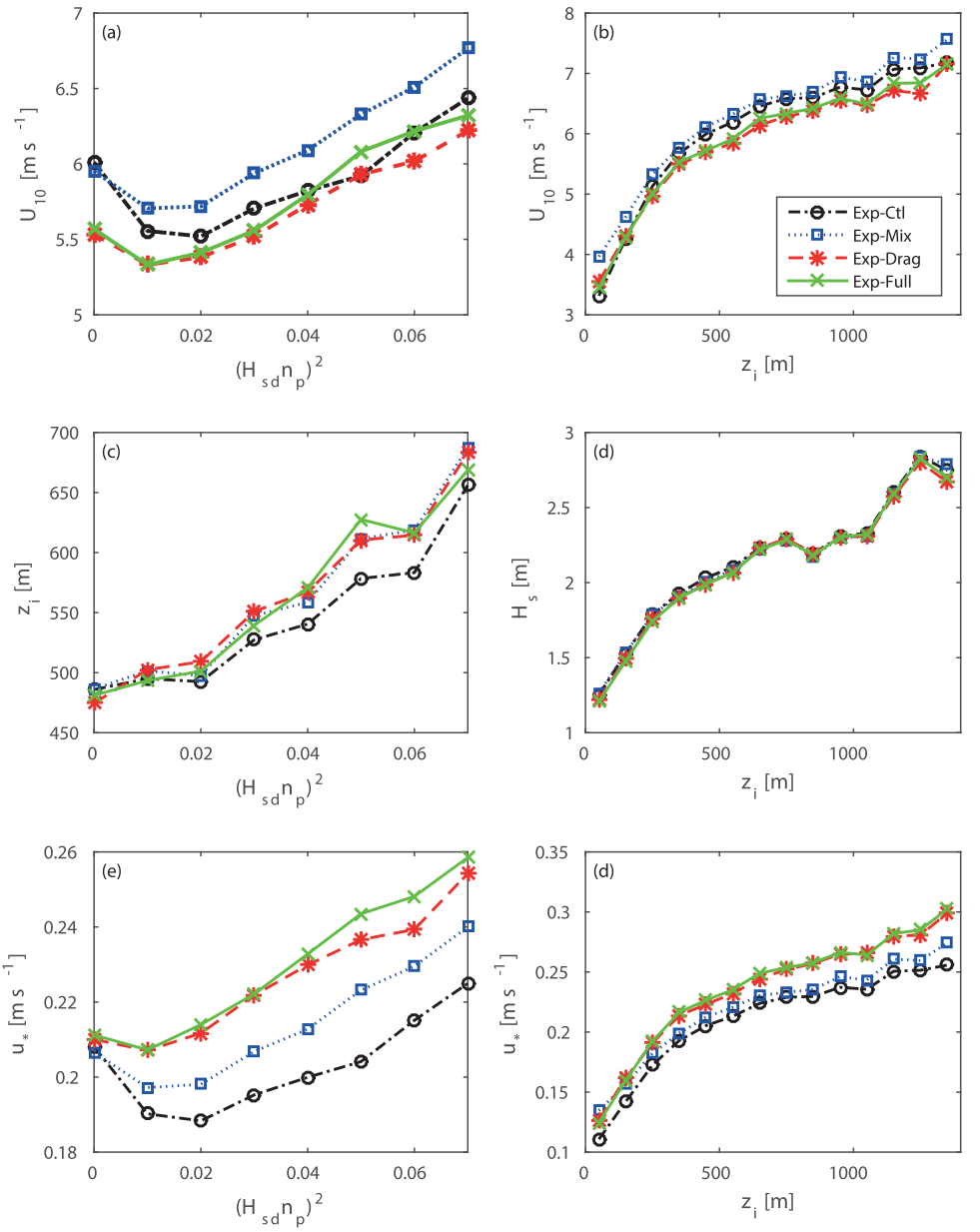

Figure 9. Average over intervals of (left columns) $(H_{sd}n_p)^2$ and (right columns) z_i from the Exp-Ctl simulations: (a, b) U_{10}, (c) z_i, (d) H_s, and (e, f) u_* for the NS in Figure 1. Circles indicate the Exp-Ctl results, rectangles the Exp-Mix results, stars the Exp-Drag results, and crosses the Exp-Ful results. Only data meeting the swell impact criteria for both atmospheric mixing length and wind stress are included.

and AT basins, the friction velocity increases with the wave parameter $(H_{sd}n_p)^2$ (Figures 7e, 8e, 9e, and 10e) and MLH (Figures 7f, 8f, 9f, and 10f) when adding the wave impact on the wind stress (Exp-Drag and Exp-Ful).

5. Discussion

In this study, we investigate the influences of swell on the wind stress and atmospheric mixing through introducing the parametrizations of *Högström et al.* [2015] and *Rutgersson et al.* [2012] into a regional coupled atmosphere-wave model. The simulations demonstrate that swell can significantly affect the simulation results, though several uncertainties remains. The lack of knowledge of atmospheric turbulence under swell conditions is the main source of uncertainty.

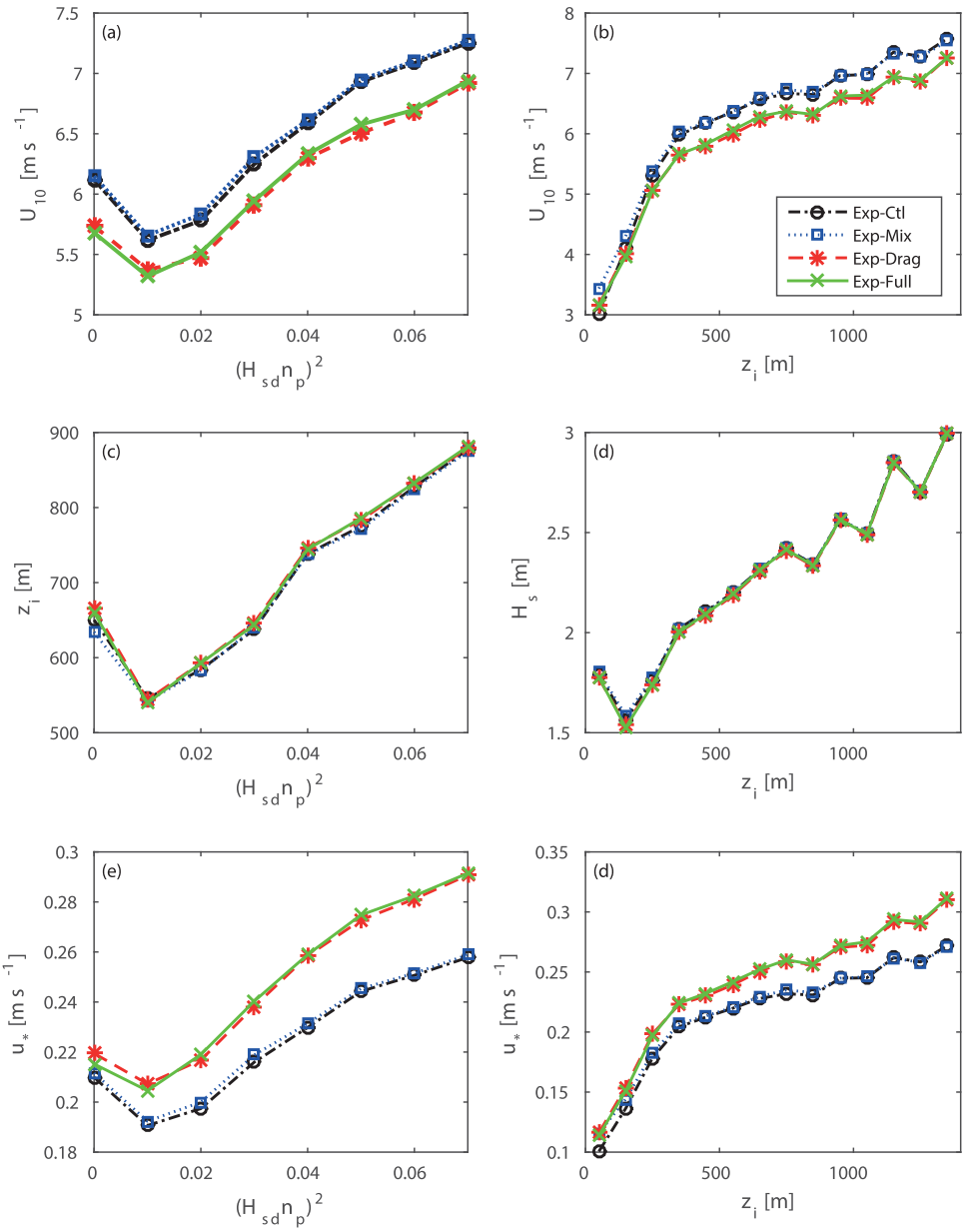

Figure 10. Average over intervals of (left columns) $(H_{sd}n_p)^2$ and (right columns) z_i from the Exp-Ctl simulations: (a, b) U_{10}, (c) z_i, (d) H_s, and (e, f) u_* for the AT in Figure 1. Circles indicate the Exp-Ctl results, rectangles the Exp-Mix results, stars the Exp-Drag results, and crosses the Exp-Ful results. Only data meeting the swell impact criteria for both atmospheric mixing length and wind stress are included.

The swell increases the atmospheric mixing, which is indicated by the LES model simulations [*Nilsson et al.*, 2012; *Rutgersson et al.*, 2012]. As expected, introducing the influence of swell on atmospheric mixing somewhat increases the wind speed at 10 m. The friction velocity then increases, caused by the increasing wind speed. The parameter for the additional mixing, W_{mix}, contributed by swell is a relatively crude tuning parameter in the parameterization (section 2.1). The value of this parameter needs more analysis and measurements before it can be used for reliable universal estimation.

Högström et al. [2015] base their wind stress parameterization on the near-neutral measurements. The turbulence determining the wind stress is in the low layer of the atmosphere, which is dominated by wave influences. Under unstable stratification conditions, swell probably still influences the wind stress. In this study, we therefore extended the parameterization to unstable stratification conditions to calculate the z_0

in the current model time step. The stability effect is taken into account in the next model time step. The new z_0 can affect the heat flux and the momentum flux. The parameterization of *Högström et al*. [2015] is based on limited measurements. More measurements are needed to verify their parameterization in certain ranges (i.e., the red area in their Figure 13). To avoid a physically unrealistically high drag coefficient, we limit the drag coefficient calculated from their parameterization, i.e., when the value of $H_{sd}^2 n_p^2$ is higher than that found in the range of the *Högström et al*. [2015] data, we used the maximum value of C_{dN} found in their data. Under swell conditions at very low wind speeds, upward momentum flux is reported [*Högström et al*., 2009]. The parameterization of *Högström et al*. [2015] is not adapted to low wind speeds. However, to avoid the sharp change in the drag coefficient in the model, the parameterization is extended to the low-wind-speed range ($U_{10} < 3.5\,\mathrm{m\,s^{-1}}$). The frequency of low-wind swell conditions is very low in the domain area and is unlikely to have a significant influence on the results.

The increase in near-surface wind speed is due to a redistribution of wind from the upper layers when adding the swell influence on the atmospheric mixing; accordingly, the friction velocity is also mostly directly increased due to this. At the same time, this redistribution can also lead to reduced wind in other regions when momentum is taken away from the upper layers. Adding the swell influence on the wind stress increases the drag coefficient when $H_{sd}^2 n_p^2$ is not very small [*Högström et al*., 2015, Figure 13]. The probability of having a small $H_{sd}^2 n_p^2$ that leads to a lower drag coefficient than in the default parameterization is very low over our study domain and periods. In general, the increased drag coefficient will cause a decrease in wind speed, as seen in the present results, because of the energy conservation principle. However, increased wind speeds are most likely if the occurrence frequency of the drag coefficient is smaller than the value resulting from the control experiment (i.e., a very small $H_{sd}^2 n_p^2$) when the swell influence on wind stress is added.

The influence of swell on atmospheric turbulence under stable and/or wind-opposing swell conditions differs from its influence under neutral or unstable stratification conditions. For this study, the parameterization of *Högström et al*. [2015] is not applied under these conditions. Under these conditions, the swell influence might also be significant, however, one could expect more influence if the swell influence were also added under those conditions. The wind stress under wind-opposing swell and stable conditions needs to be studied further.

Adding the influences of swell on the atmospheric mixing or/and wind stress has a little effect on the simulation results of the wave parameters, possibly because that the WAM gets only the wind field from the RCA model. The measurements used in the comparison come from the coastal area, where the wind speed differs very little between experiments. The wind speed differences are not large enough to change the wave simulation results significantly. The simulation results do not improve at high wind speeds, possibly because the sea spray generated at these speeds exerts a very important reducing effect on the drag coefficient, an effect not included in the parameterization [*Wu et al*., 2015].

In our current model simulation domain, the swell frequency is lower than in low-latitude oceans. In the high frequency swell areas, the swell should therefore have considerable influence compared with the low frequency swell areas on the simulation results. For the global atmospheric circulation, the difference in the influences will also play a role in global climate simulations.

6. Conclusions

Measurements and LES results indicate that swell can significantly influence the atmospheric turbulence structure; it then influences the wind stress, atmospheric mixing, etc. Under swell conditions, the atmospheric mixing length increases because of the change in atmospheric turbulence. The drag coefficient is related not only to wind speed, but also to wave states. In the present study, we applied an atmospheric mixing-length parameterization [*Rutgersson et al*., 2012] and wind stress parameterization [*Högström et al*., 2015] to an atmosphere-wave-coupled model (RCA-WAM) under swell conditions. Based on a 5 year simulation, we studied the influences of swell.

Adding the swell influence on the wind stress and/or atmospheric mixing improves the model performance concerning the wind speed ($U_{10} < 8\,\mathrm{m\,s^{-1}}$) relative to measurements. At high wind speeds, adding the swell influence does not have a significant effect. Adding the swell influence on both atmospheric mixing

and wind stress (Exp-Full) results in the best performance in terms of wind speed. Adding the swell influence on atmospheric mixing (Exp-Mix) slightly increases the average U_{10} over the ocean. In contrast, adding the swell influence on wind stress (Exp-Drag) reduces the average U_{10}. The influence of swell on wind stress (Exp-Drag) is greater than the influence of atmospheric mixing (Exp-Mix). Adding the swell influence increases the friction velocity in all the experiments, i.e., Exp-Mix, Exp-Drag, and Exp-Full.

The impact varies between regions because of their different wave characteristics. We conclude that the swell influences on both atmospheric mixing and wind stress should be taken into account when developing weather forecasting and climate models.

Acknowledgments
Lichuan Wu is supported by the Swedish Research Council (project 2012-3902). The data used in this study can be acquired by contacting the first author (wulichuan0704@gmail.com).

References

Carlsson, B., A. Rutgersson, and A.-S. Smedman (2009), Impact of swell on simulations using a regional atmospheric climate model, *Tellus, Ser. A*, *61*(4), 527–538.
Cuxart, J., P. Bougeault, and J.-L. Redelsperger (2000), A turbulence scheme allowing for mesoscale and large-eddy simulations, *Q. J. R. Meteorol. Soc.*, *126*(562), 1–30.
Drennan, W. M., H. C. Graber, and M. A. Donelan (1999a), Evidence for the effects of swell and unsteady winds on marine wind stress, *J. Phys. Oceanogr.*, *29*(8), 1853–1864.
Drennan, W. M., K. K. Kahma, and M. A. Donelan (1999b), On momentum flux and velocity spectra over waves, *Boundary Layer Meteorol.*, *92*(3), 489–515.
Drennan, W. M., P. K. Taylor, and M. J. Yelland (2005), Parameterizing the sea surface roughness, *J. Phys. Oceanogr.*, *35*(5), 835–848.
Fairall, C., E. F. Bradley, J. Hare, A. Grachev, and J. Edson (2003), Bulk parameterization of air-sea fluxes: Updates and verification for the COARE algorithm, *J. Clim.*, *16*(4), 571–591.
García-Nava, H., F. Ocampo-Torres, P. Osuna, and M. Donelan (2009), Wind stress in the presence of swell under moderate to strong wind conditions, *J. Geophys. Res.*, *114*, C12008, doi:10.1029/2009JC005389.
Grachev, A., and C. Fairall (2001), Upward momentum transfer in the marine boundary layer, *J. Phys. Oceanogr.*, *31*(7), 1698–1711.
Guan, C., and L. Xie (2004), On the linear parameterization of drag coefficient over sea surface, *J. Phys. Oceanogr.*, *34*(12), 2847–2851.
Hanley, K. E., and S. E. Belcher (2008), Wave-driven wind jets in the marine atmospheric boundary layer, *J. Atmos. Sci.*, *65*(8), 2646–2660.
Högström, U., et al. (2008), Momentum fluxes and wind gradients in the marine boundary layer: A multi platform study, *Boreal Environ. Res.*, *13*(6), 475–502.
Högström, U., A. Smedman, E. Sahleé, W. Drennan, K. Kahma, H. Pettersson, and F. Zhang (2009), The atmospheric boundary layer during swell: A field study and interpretation of the turbulent kinetic energy budget for high wave ages, *J. Atmos. Sci.*, *66*(9), 2764–2779.
Högström, U., A. Rutgersson, E. Sahlée, A.-S. Smedman, T. S. Hristov, W. Drennan, and K. Kahma (2013), Air–sea interaction features in the Baltic Sea and at a pacific trade-wind site: An inter-comparison study, *Boundary Layer Meteorol.*, *147*(1), 139–163.
Högström, U., E. Sahleé, A. Smedman, A. Rutgersson, E. Nilsson, K. K. Kahma, and W. M. Drennan (2015), Surface stress over the ocean in swell-dominated conditions during moderate winds, *J. Atmos. Sci.*, *66*(9), 2764–2779.
Kudryavtsev, V., and V. Makin (2004), Impact of swell on the marine atmospheric boundary layer, *J. Phys. Oceanogr.*, *34*(4), 934–949.
Larsén, X. G., V. K. Makin, and A.-S. Smedman (2003), Impact of waves on the sea drag: Measurements in the Baltic Sea and a model interpretation, *Global Atmos. Ocean Syst.*, *9*(3), 97–120.
Lenderink, G., and W. De Rooy (2000), A robust mixing length formulation for a TKE-l turbulence scheme, *Hirlam Newsl.*, *36*, 25–29.
Lenderink, G., and A. A. Holtslag (2004), An updated length-scale formulation for turbulent mixing in clear and cloudy boundary layers, *Q. J. R. Meteorol. Soc.*, *130*(604), 3405–3428.
Nilsson, E. O., A. Rutgersson, A.-S. Smedman, and P. P. Sullivan (2012), Convective boundary-layer structure in the presence of wind-following swell, *Q. J. R. Meteorol. Soc.*, *138*(667), 1476–1489.
Potter, H. (2015), Swell and the drag coefficient, *Ocean Dyn.*, *65*(3), 375–384.
Rutgersson, A., A.-S. Smedman, and U. Högström (2001), Use of conventional stability parameters during swell, *J. Geophys. Res.*, *106*(C11), 27,117–27,134.
Rutgersson, A., Ø. Sætra, A. Semedo, B. Carlsson, and R. Kumar (2010), Impact of surface waves in a regional climate model, *Meteorol. Z.*, *19*(3), 247–257.
Rutgersson, A., E. Nilsson, and R. Kumar (2012), Introducing surface waves in a coupled wave-atmosphere regional climate model: Impact on atmospheric mixing length, *J. Geophys. Res.*, *117*, C00J15, doi:10.1029/2012JC007940.
Sahlée, E., W. M. Drennan, H. Potter, and M. A. Rebozo (2012), Waves and air-sea fluxes from a drifting ASIS buoy during the Southern Ocean Gas Exchange experiment, *J. Geophys. Res.*, *117*, C08003, doi:10.1029/2012JC008032.
Semedo, A., Ø. Saetra, A. Rutgersson, K. K. Kahma, and H. Pettersson (2009), Wave-induced wind in the marine boundary layer, *J. Atmos. Sci.*, *66*(8), 2256–2271.
Semedo, A., K. Sušelj, A. Rutgersson, and A. Sterl (2011), A global view on the wind sea and swell climate and variability from era-40, *J. Clim.*, *24*(5), 1461–1479.
Smedman, A., U. Högström, H. Bergström, A. Rutgersson, K. Kahma, and H. Pettersson (1999), A case study of air-sea interaction during swell conditions, *J. Geophys. Res.*, *104*(C11), 25,833–25,851.
Smedman, A., U. Högström, E. Sahlée, W. Drennan, K. Kahma, H. Pettersson, and F. Zhang (2009), Observational study of marine atmospheric boundary layer characteristics during swell, *J. Atmos. Sci.*, *66*(9), 2747–2763.
Smedman, A.-S., M. Tjernström, and U. Högström (1994), The near-neutral marine atmospheric boundary layer with no surface shearing stress: A case study, *J. Atmos. Sci.*, *51*(23), 3399–3411.
Smedman, A.-S., X. Guo Larsén, U. Högström, K. K. Kahma, and H. Pettersson (2003), Effect of sea state on the momentum exchange over the sea during neutral conditions, *J. Geophys. Res.*, *108*(C11), 3367, doi:10.1029/2002JC001526.
Sullivan, P. P., J. B. Edson, T. Hristov, and J. C. McWilliams (2008), Large-eddy simulations and observations of atmospheric marine boundary layers above nonequilibrium surface waves, *J. Atmos. Sci.*, *65*(4), 1225–1245.
Taylor, P. K., and M. J. Yelland (2001), The dependence of sea surface roughness on the height and steepness of the waves, *J. Phys. Oceanogr.*, *31*(2), 572–590.

Troen, I., and L. Mahrt (1986), A simple model of the atmospheric boundary layer; sensitivity to surface evaporation, *Boundary Layer Meteorol.*, *37*(1–2), 129–148.
Uppala, S. M., et al. (2005), The era-40 re-analysis, *Q. J. R. Meteorol. Soc.*, *131*(612), 2961–3012.
Valcke, S. (2013), The OASIS3 coupler: a European climate modelling community software, *Geosci. Model. Dev.*, *6*, 373–388, doi:10.5194/gmd-6-373-20-13.
Veron, F., W. K. Melville, and L. Lenain (2008), Wave-coherent air-sea heat flux, *J. Phys. Oceanogr.*, *38*(4), 788–802.
WAMDI (1988), The WAM model-a third generation ocean wave prediction model, *J. Phys. Oceanogr.*, *18*(12), 1775–1810.
Wu, L., A. Rutgersson, E. Sahlée, and X. G. Larsén (2015), The impact of waves and sea spray on modelling storm track and development, *Tellus, Ser. A*, *67*, 27,967.